




# Top quark mass measurements at the $t\bar{t}$ threshold with CEPC

Zhan Li<sup>1,2</sup>, Xiaohu Sun<sup>3,a</sup> , Yaquan Fang<sup>1,2,b</sup>, Gang Li<sup>1,2</sup>, Shuiting Xin<sup>1,2</sup>, Shudong Wang<sup>1,2</sup>, Yiwei Wang<sup>1,2</sup>, Yuan Zhang<sup>1,2</sup>, Hao Zhang<sup>1,2,4</sup>, Zhijun Liang<sup>1,2</sup>

<sup>1</sup> Institute of High Energy Physics, 19B, Yuquan Road, Shijingshan District, Beijing 100049, China

<sup>2</sup> University of Chinese Academy of Sciences (CAS), 19A, Yuquan Road, Shijingshan District, Beijing 100049, China

<sup>3</sup> Department of Physics and State Key Laboratory of Nuclear Physics and Technology, Peking University, 209 Chengfu Road, Haidian District, Beijing 100871, China

<sup>4</sup> Center for High Energy Physics, Peking University, 209 Chengfu Road, Haidian District, Beijing 100871, China

Received: 15 August 2022 / Accepted: 17 March 2023 / Published online: 1 April 2023  
© The Author(s) 2023, corrected publication 2023

**Abstract** We present a study of top quark mass measurements at the  $t\bar{t}$  threshold based on CEPC. A centre-of-mass energy scan near two times of the top quark mass is performed and the measurement precision of top quark mass, width and  $\alpha_S$  are evaluated using the  $t\bar{t}$  production rates. Realistic scan strategies at the threshold are discussed to maximise the sensitivity to the measurements individually and simultaneously in the CEPC scenarios assuming a total luminosity limited to  $100 \text{ fb}^{-1}$ . With the optimal scan for individual property measurements, the top quark mass precision is expected to be 9 MeV, the top quark width precision is expected to be 26 MeV, and  $\alpha_S$  can be measured at a precision of 0.00039, considering only the statistical uncertainty. Taking into account the systematic uncertainties from theory, width,  $\alpha_S$ , experimental efficiency, background subtraction, beam energy and luminosity spectrum, the top quark mass can be measured at a precision of 25 MeV optimistically and 59 MeV conservatively at CEPC.

## 1 Introduction

Top quark, the heaviest fundamental particle observed so far, plays an important role in the Standard Model (SM). It provides the strongest coupling to the SM Higgs boson and opens doors to new physics beyond the SM (BSM). Till now, the top quark mass have only been measured at hadron collisions, e.g. the Tevatron and the Large Hadron Collider (LHC), using the direct reconstruction of the invariant mass of the top quark decay products. In future electron–positron colliders the top quark mass can be measured not only by the direct recon-

struction but also by a scan on the centre-of-mass energy at the  $t\bar{t}$  threshold. The cross-section of  $t\bar{t}$  increases sharply as the centre-of-mass energy goes through the  $t\bar{t}$  threshold and depends strongly on the top quark mass, width and  $\alpha_S$ , which provides a sensitive probe to these measurements. This is the so-called threshold-scan method that was discussed for top quark mass measurements at an electron–positron collider [1–4].

In experiments, the top quark mass has been measured by using the direct reconstruction of the top quark decay products as  $174.30 \pm 0.35$  (stat.)  $\pm 0.54$  (syst.) GeV from the combined results of CDF and D0 at Tevatron [5],  $172.69 \pm 0.25$  (stat.)  $\pm 0.41$  (syst.) GeV with ATLAS [6] and  $172.44 \pm 0.13$  (stat.)  $\pm 0.47$  (syst.) GeV with CMS [7] at the LHC. The precision till now is about half a GeV and it is mainly limited by the systematic uncertainties that are not easily reduced in the future. On the contrary, the threshold-scan method has been widely used [8,9] and shown good performance with a statistical uncertainty of top quark mass measurement at  $\mathcal{O}(10)$  MeV that was studied previously with ILC, CLIC and FCC-ee [10–14].

The threshold-scan method also provides a theoretically well defined mass that can be calculated with a high degree of precision and can be easily converted to various theoretical schemes. This is difficult to be realised in the reconstructed top quark mass peak method in which the generated mass peak is usually used as a template to fit to the observed data. The recent progresses in the interpretation of the reconstructed top quark mass measurements are reviewed in Ref. [15].

In this article, we discuss the threshold-scan method and propose realistic scan strategies for the top quark mass measurements with electron–positron collisions based on the Circular Electron Positron Collider (CEPC). The experimental

<sup>a</sup> e-mail: [Xiaohu.Sun@pku.edu.cn](mailto:Xiaohu.Sun@pku.edu.cn) (corresponding author)

<sup>b</sup> e-mail: [fangyq@ihep.ac.cn](mailto:fangyq@ihep.ac.cn)

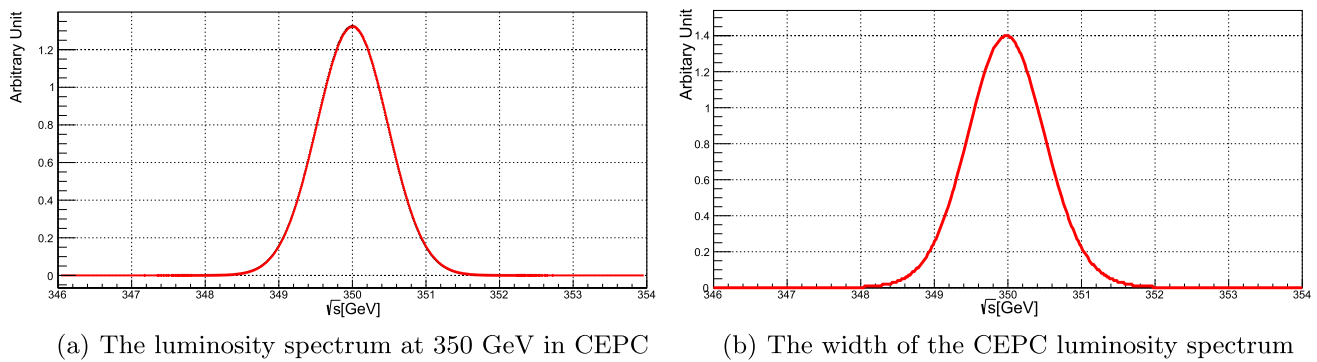


**Fig. 1** The luminosity spectrum of CEPC and its width that increases as a function of the centre-of-mass energy

conditions at CEPC are introduced in Sect. 2. The threshold-scan method applied to the CEPC scenarios, the likelihood and the Fisher information are introduced in Sect. 3. The extraction of one parameter at a time, i.e. top quark mass, width or  $\alpha_S$ , is discussed in Sect. 4, while the extraction of two parameters at a time is discussed in Sect. 5. The systematic uncertainties from the theoretical calculation on the cross-section,  $\alpha_S$ , width, the beam energy, the luminosity spectrum and the background contamination are discussed in Sect. 6. Eventually the conclusions are presented in Sect. 7.

## 2 Experimental conditions at CEPC

CEPC is a large concept collider with a circumference of 100 km and two interaction points [16, 17]. The accelerator complex consists of a linear accelerator (Linac), a damping ring (DR), the booster, the collider and several transport lines. The centre-of-mass energy of CEPC will be 240 GeV, at which collision energy it will serve as a Higgs factory, generating more than one million Higgs particles corresponding to a total luminosity of  $5.6 \text{ ab}^{-1}$  as a baseline design. The design also allows operation at 91 GeV for a Z factory and at 160 GeV for the  $W^+W^-$  threshold scan. The number of Z particles will be close to 1 trillion from  $16 \text{ ab}^{-1}$  data taking, and  $W^+W^-$  pairs about 15 million from  $2.6 \text{ ab}^{-1}$  data taking. These unprecedented large number of particles make the CEPC a powerful instrument not only for precision measurements on these fundamental particles, but also in the search for new physics. Apart from those, CEPC could also ramp up the centre-of-mass energy to reach the  $t\bar{t}$  threshold with a preliminary plan to collect a total luminosity of  $100 \text{ fb}^{-1}$ .

Unlike linear colliders, circular colliders have bending magnets in the acceleration ring, which help to constrain the beam energy spread. Thus, the luminosity spectrum (LS) is more concentrated at the beam energy peak. The spread of LS increases as the centre-of-mass energy rises. At CEPC, LS is modeled by a Gaussian distribution and its width  $\sigma_{LS}$

is a function of centre-of-mass energy  $\sqrt{s}$ :

$$\sigma_{LS} = 0.51 \times \left( \frac{\sqrt{s}}{360} \right)^2 \quad (1)$$

which is shown in Fig. 1. The width  $\sigma_{LS}$  is roughly 500 MeV around the  $t\bar{t}$  threshold, resulting in a luminosity spectrum with more than 90% of the collisions in the top 1% of the energy at 350 GeV, compared to 77% of that in the top 1% at CLIC, at the same energy [18, 19].

## 3 Analysis setup

The package QQbar\_threshold (VERSION 2.2.0) is used [20, 21] to calculate the  $t\bar{t}$  cross-section around the threshold. The potential-subtracted (PS) scheme is used for the top quark mass,  $m_{top}^{PS} = 171.5 \text{ GeV}$ . The width is set to 1.33 GeV and the strong coupling  $\alpha_S$  to 0.1184. The cross-section is calculated in next-to-next-to-next-to-leading order ( $N^3\text{LO}$ ) QCD in resummed non-relativistic perturbation theory [22, 23] and next-to-next-to-leading order (NNLO) in electroweak [21]. Two important beam effects, e.g. the initial state radiation (ISR) and the LS that is a function of centre-of-mass energy based on the CEPC scenario, are both taken into account with QQbar\_threshold.

The cross-section as a function of centre-of-mass energy is shown in Fig. 2 including the calculation without ISR or LS, the one with ISR and the one with both ISR and LS. The original cross-section curve is significantly worn down by the two effects.

The number of  $t\bar{t}$  events are calculated with the cross-section that is a function of top quark mass, width and  $\alpha_S$ , and the corresponding luminosity assumed for the centre-of-mass energy in the scan. The semi-leptonic and full-hadronic decay modes are taken into account. The signal efficiency and acceptance follow the same as evaluated in Ref. [11]. The background contribution is relatively low and can be subtracted as discussed in Ref. [11]. The background is neglected

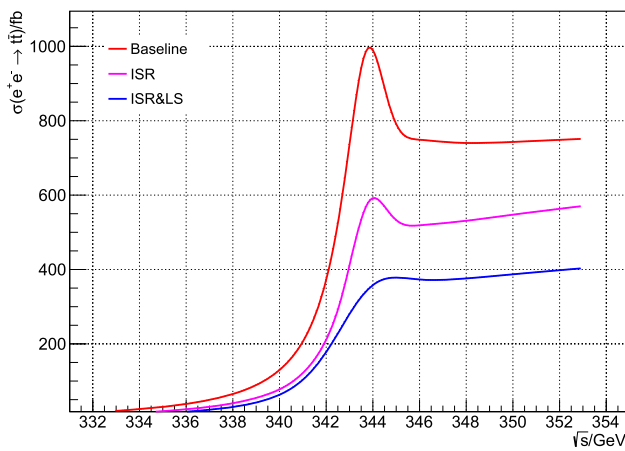


**Fig. 2** The  $t\bar{t}$  cross-section as a function of centre-of-mass energy calculated from  $Q\bar{Q}$  threshold including the cross-section values without ISR or LR (baseline), the ones with ISR only and the ones with both ISR and LS

for the nominal estimations, but its impact will be discussed as systematic uncertainties later in Sect. 6.

To extract the top quark mass, width and  $\alpha_S$ , the number of events are counted at each centre-of-mass energy in the scan. A likelihood function is constructed to perform the fits with the counted numbers, between the expected number of events evaluated with the cross-section turn-on curve and the observed number of events from the CEPC. The latter number is simply set equal to the former to make the nominal evaluation and estimate the measurement precision, i.e. the  $1\sigma$  error in the likelihood curve. The likelihood function is defined as

$$\mathcal{L} = \prod_{i=1}^N P(D|\sigma_{t\bar{t}}(m_{top}, \Gamma_{top}, \alpha_S, \sqrt{s_i}) \times L_i \times \epsilon), \quad (2)$$

where the observed number of events ( $D$ ) should follow the Poissonian distribution with the expected mean as  $E = \sigma_{t\bar{t}}(m_{top}, \Gamma_{top}, \alpha_S, \sqrt{s_i}) \times L \times \epsilon$  under certain centre-of-mass energy ( $\sqrt{s_i}$  indexed with  $i$ ). The likelihood function combines all  $N$  energy points by multiplying all the Poissonian probability  $P$  of each collision energy. In the equation,  $\sigma_{t\bar{t}}$  stands for the cross-section,  $m_{top}$  for the top quark mass,  $\Gamma_{top}$  for the top quark width,  $\alpha_S$  for the strong coupling,  $L_i$  for the luminosity allocated to the collisions at the centre-of-mass energy of  $\sqrt{s_i}$ , and  $\epsilon$  for the selection efficiency times acceptance of the  $t\bar{t}$  signal events. The precision of measurement on  $m_{top}$ ,  $\Gamma_{top}$ , and  $\alpha_S$  is evaluated by minimising the negative log likelihood function.

The cross-section curve contains different amounts of information at different the centre-of-mass energy scan points, for top quark mass, width and  $\alpha_S$ . One needs to find out what level of sensitivity the cross-section curve can pro-

vide for the measurements. The Fisher information is used here as a rule of thumb. At a certain centre-of-mass energy ( $\sqrt{s}$ ) one can consider the measured cross-section ( $\sigma$ ) as a random variable which follows a Gaussian distribution ( $G$ ) with its mean value centred at the true cross-section ( $\sigma_0(\sqrt{s}, \theta)$ ), where  $\theta$  can be top quark properties like top quark mass  $m_{top}$  and width  $\Gamma_{top}$  as well as the strong coupling  $\alpha_S$ , and its width ( $\sqrt{\sigma_0(\sqrt{s}, \theta)}$ ). Thus the Fisher information reads

$$I(\sqrt{s}) = \int \left( \frac{\partial \log(G(\sigma|\sigma_0(\sqrt{s}, \theta), \sqrt{\sigma_0(\sqrt{s}, \theta)}))}{\partial \theta} \right)^2 \times G(\sigma|\sigma_0(\sqrt{s}, \theta), \sqrt{\sigma_0(\sqrt{s}, \theta)}) d\sigma. \quad (3)$$

In this way, the Fisher information can reflect the sensitivity to the measurements of top quark mass, width and  $\alpha_S$  as a function of centre-of-mass energy, respectively, as shown in Fig. 3. The larger the value in the Y-axis of the Fisher information is, the more sensitive to the relevant measurement the cross-section at this centre-of-mass energy would be. The cross-section curve is found most sensitive to top quark mass when the cross-section ramps up around the threshold, and is sensitive to top quark width when the cross-section peaks, while it is sensitive to  $\alpha_S$  by its overall rate thus mainly close to the cross-section peak.

The effects of ISR and LS wear out the original cross-section curve resulting significant drops in Fisher information for all three parameters as shown in Fig. 3. Considering the ISR effect only, collisions at  $\sqrt{s} = 343.00$  GeV provide the highest sensitivity to the top quark mass,  $\sqrt{s} = 343.75$  GeV for top quark width and  $\sqrt{s} = 343.25$  GeV for  $\alpha_S$ . Considering both ISR and LS effects, the optimal energy points are shifted. Then collisions at  $\sqrt{s} = 342.75$  GeV provide the highest sensitivity to the top quark mass measurements,  $\sqrt{s} = 344.00$  GeV for top quark width, and  $\sqrt{s} = 343.50$  GeV for  $\alpha_S$ .

#### 4 Extraction of one parameter

In this section, the extraction of one parameter at a time is discussed, i.e. top quark mass, width or  $\alpha_S$ , while the other two are fixed to their predictions in the SM. With the total luminosity assumed up to  $100 \text{ fb}^{-1}$ , the optimal scan strategy is discussed with only statistical uncertainty, while detailed systematic uncertainties are presented in Sect. 6. The first question is how many energy points are optimal for the extraction of one parameter assuming the total luminosity fixed. The study with the total luminosity evenly allocated with different numbers of centre-of-mass energy scan point is then performed. Using the Fisher information as a guide, one can

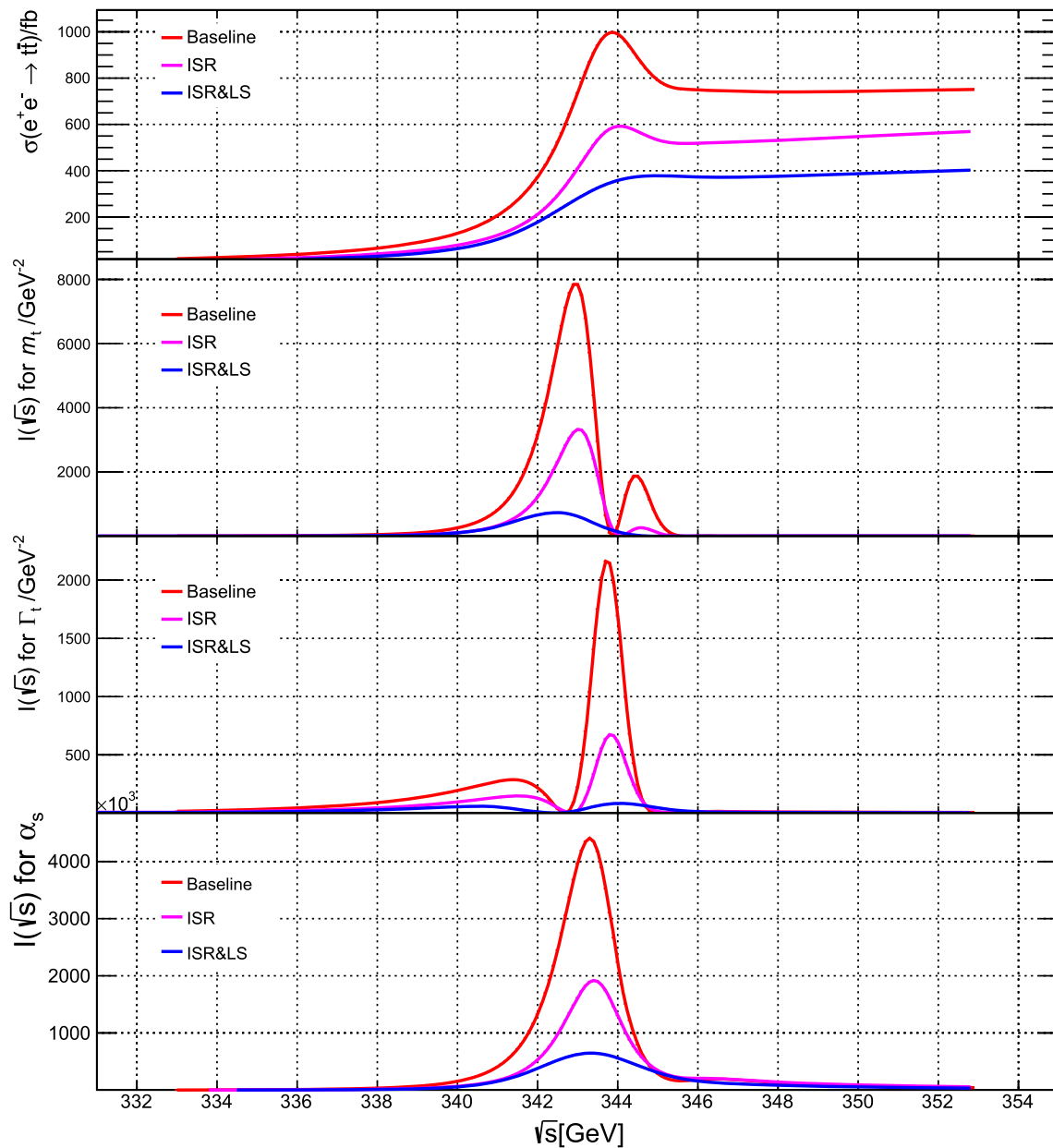


**Fig. 3** The Fisher information for top quark mass, width and  $\alpha_s$  along the centre-of-mass energy around the  $t\bar{t}$  threshold. The baseline curves are calculated without ISR or LR. The ISR curves are calculated with ISR only, while the ISR and LS curves are calculated with both ISR and LS

propose various grids of collision energy and evaluate the sensitivities. The following grids are tested.

- 8-point grid: {341, 342, 342.5, 342.75, 343, 343.5, 344.5, 345} GeV
- 6-point grid: {342, 342.5, 342.75, 343, 343.5, 344.5} GeV
- 4-point grid: {342.5, 342.75, 343, 343.5} GeV
- 1-point grid: {342.75} GeV

among which the energy point most sensitive to top quark mass is always included. The likelihood function defined in Eq. 2 is calculated for each scan grid and the error at 68% confidence level in the likelihood scan is taken as the statistical uncertainty. The uncertainties on top quark mass measurement are 13 MeV from 8 energy points, 12 MeV from 6 energy points, 10 MeV from 4 energy points and 9 MeV from 1 energy point. Therefore, when allocating luminosity evenly to the centre-of-mass energy points in the scan, the optimal solution is to take all the data at the energy point that is most sensitive to top quark mass given that the opti-

**Table 1** The negative log likelihood (NLL) value for several top quark mass (170.6 GeV, 171.1 GeV, 171.6 GeV, 172.1 GeV and 172.6 GeV) in a low-luminosity scan (1 fb<sup>-1</sup> per energy point)

$m_{top}$ (GeV)	NLL
170.6	16.1
171.1	12.2
171.6	6.2
172.1	24.0
172.6	51.5

The smallest NLL value should point to  $m_{top}$  closest to the true one

mal energy point is known. Further tests are performed for unevenly allocating the luminosity around the optimal energy point, the conclusion does not change.

In practice, the optimal energy point is unknown. One can perform a quick scan with low-luminosity (1 fb<sup>-1</sup> per energy point) to get close to the true optimal point. The cross-section dependence on the top quark mass is assumed, which is the same as used in the full-luminosity scan described above. Two steps are needed, firstly for identifying the  $m_{top}$  value that is as close as possible to the true  $m_{top}$  to nail down the theoretical prediction of the cross-section curve, and secondly for locating the optimal energy point using the the cross-section curve.

In the first step of the quick scan, one approaches the true  $m_{top}$  value by fitting the theoretical prediction of the  $t\bar{t}$  cross-section to the real data with a couple of collision energy points. The scan range of  $m_{top}$  can benefit from the knowledge of the LHC (or HL-LHC) data that will provide the interval of the top quark mass at a certain confidence level. Here, we assume  $m_{top} = 171.5$  GeV as the true value for the real data taken under the energy points of  $\sqrt{s} = \{340, 341, 342, 343, 344, 345\}$  which can be re-used in the next step. A likelihood function constructed with the cross-section prediction and the real data is calculated as a function of top mass using all the above energy points simultaneously, from which one can identify the  $m_{top}$  that is closest to the true value. Some of them are listed in Table 1 for mass points of 170.6 GeV, 171.1 GeV, 171.6 GeV, 172.1 GeV and 172.6 GeV. The one that leads to the smallest negative log likelihood (NLL) value is the one closest to the true value. One can certainly minimise the likelihood with finer scans on  $m_{top}$  to get as close as possible to the true  $m_{top}$ .

In the second step, one quickly scans on the energy points with low luminosity (1 fb<sup>-1</sup> per energy point) to approach the optimal energy point for the full-luminosity measurement later. From each energy point in the quick scan, one locates the energy point most closest to the optimal point by looking at their precision on the top mass individually. Here, let's re-use the data taken from the energy grid above  $\sqrt{s} = \{340, 341, 342, 343, 344, 345\}$ . As listed in Table 2, the

**Table 2** The uncertainty of top quark mass measurement in a low-luminosity scan (1 fb<sup>-1</sup> per energy point)

$\sqrt{s}$ (GeV)	$\Delta m_{top}$ (MeV)
343	100.2
342	108.4
341	176.0

The centre-of-mass energies of {340, 341, 342, 343, 344, 345} are scanned. The scan points are ordered with the measured top quark mass precision. Only the first three are listed in the table

**Table 3** The uncertainty of top quark mass measurement in a low-luminosity scan (1 fb<sup>-1</sup> per energy point)

$\sqrt{s}$ (GeV)	$\Delta m_{top}$ (MeV)
342.75	93.7
342.50	94.0
343.00	100.2

The centre-of-mass energies of {342.25, 342.5, 342.75, 343, 343.25, 343.5} are scanned. The scan points are ordered with the measured top quark mass precision. Only the first three are listed in the table

**Table 4** The statistical uncertainties of the measurements of top quark mass, width and  $\alpha_S$  measured individually at their optimal energy points that can be determined with a quick scan using low luminosity

$\sqrt{s}$ (GeV)	$\Delta m_{top}$	$\Delta \Gamma_{top}$	$\Delta \alpha_S$
342.75	9 MeV	343 MeV	0.00041
344.00	> 50 MeV	26 MeV	0.00047
343.50	15 MeV	40 MeV	0.00040

In the table, 342.75 GeV, 344.00 GeV and 343.50 GeV are optimal energy points for top quark mass, width and  $\alpha_S$ , respectively

scan points are ordered with the measured top quark mass precision. From that, one can conclude that the optimal energy point should sit between 342 GeV and 343 GeV. Then a finer grid between 342 GeV and 343 GeV,  $\sqrt{s} = \{342.25, 342.5, 342.75, 343, 343.25, 343.5\}$ , can be scanned, again with even luminosity of 1 fb<sup>-1</sup> per energy point, as shown in Table 3. From that, one can get closer to the optimal energy point. This process can be iterated with more times to get close enough to the best energy point. Alternatively, the optimal energy point could also be located by calculating the Fisher information out of the cross-section curve.

With the CEPC setup, the ultimate statistical precision is calculated individually for top quark mass, width and  $\alpha_S$  at their optimal energy points that can be determined with a quick scan using low luminosity, respectively, assuming the total luminosity of 100 fb<sup>-1</sup> for each case. The statistical uncertainties of these measurements are listed in Table 4. Relevant systematic uncertainties are discussed in Sect. 6.



## 5 Extraction of two parameters

In this section, the extraction of two parameters simultaneously is discussed. Given that top quark mass is of great interests, the studies always include it and are performed on the extractions of top quark mass vs  $\alpha_S$  and of top quark mass vs width. The energy point that is optimal for top quark mass is taken and to give sufficient constraints on two parameter at a time one more energy point needs to be added.

To find out that point, the cross-section and the likelihood are calculated in the two-dimensional planes. Figure 4 (left column) shows the cross-section at a certain energy point on the plane of top quark mass vs  $\alpha_S$ , which assists to understand the likelihood calculated at the corresponding single energy point in Fig. 4 (right column). Figure 5 shows the same but on the plane of top quark mass vs width.

To keep high sensitivity to top quark mass, the optimal energy point 342.75 GeV as suggested by the Fisher information in Fig. 3 is used. Naively the second energy point to use in the scan of top quark mass vs  $\alpha_S$  would be 343.50 GeV which is optimal for  $\alpha_S$ , but it is too close to the optimal point for top quark mass 342.75 GeV. This makes the cross-section curve highly sensitive to both parameters, leading to both variations dominating the cross-section uncertainty (roughly reading  $\Delta\sigma \propto \sqrt{A\Delta m_t^2 + B\Delta\alpha_S^2}$ ). This results in a strong correlation between top quark mass and  $\alpha_S$ , as shown in Fig. 4d. This contour is almost parallel to the one in Fig. 4b. The combination of the two, i.e. a simultaneous fit using the two energy points, would leave the contour open in the diagonal. Therefore, one has to drop the optimal point for  $\alpha_S$  and move higher to somewhere the cross-section curve still keep some sensitivity to it but leaves much less constraint power on top quark mass. The energy point 344.50 GeV is one of these points in tests and shows the best performance. Figure 4f refers to this energy and shows a clear different correlation than Fig. 4b. The resulting contour of the combined Fig. 4b, f would then close in the diagonal.

Following the same optimisation strategy, finding the second energy point for top quark mass vs width is simpler. In Fig. 3 (lines marked as “ISR and LS”), the cross-section curve have the best sensitivity for top quark mass and width at two far enough energy points, and these two points have either high sensitivity in top quark mass while low in width, or the opposite. The energy point of 342.75 GeV has a strong constraint on top quark mass, but not on much on width, while 344.00 GeV then constrains strongly the width but is almost insensitive to top quark mass, as shown in Fig. 5d, f. The combination of the two energy points yields meaningful results in both parameters.

Figure 6 shows the two-dimensional fit for top quark mass vs  $\alpha_S$ , while Fig. 7 for top quark mass vs width, both using the two energy points chosen in the above procedure. The

uncertainty is 28 MeV on top quark mass and 0.00106 on  $\alpha_S$  in the simultaneous fit of the two parameters using the energy points of 342.75 and 344.50 GeV. The uncertainty is 27 MeV on top quark mass and 72 MeV on width in the simultaneous fit of the two parameters using the energy points of 342.75 and 344.00 GeV.

So far, the two energy points split the total luminosity evenly, i.e. 50% vs 50%. Thus, an additional check on the uneven split of the luminosity is performed in Fig. 8 for top quark mass vs  $\alpha_S$  and in Fig. 9 for top quark mass vs width. Figure 8 presents the sensitivities by varying luminosity fractions of 80% vs 20%, 60% vs 40%, 50% vs 50%, 40% vs 60% and 20% vs 80% on the energy points of 342.75 GeV and 344.50 GeV used in top quark mass and  $\alpha_S$  scan, while Fig. 9 does the similar tests but for the energy points of 342.75 GeV and 344.00 GeV used in top quark mass and width scan. Figure 8 suggests that the 50–50% split is optimal for top quark mass and sub-optimal for  $\alpha_S$ . Moving more luminosities from 342.75 to 344.50 GeV (such as the split of 20% vs 80%) can slightly improve the precision on  $\alpha_S$  but will lose a lot in top quark mass. Figure 9 suggests that from 50% vs 50% to 80% vs 20% there is a sizeable improvement in top quark mass, but it degrades the width precision too much. The split of 50% vs 50% can a pragmatic choice for both.

## 6 Systematic uncertainties

The threshold-scan method depends on the theoretical calculation of the cross-section curve as a function of the centre-of-mass energy. The uncertainty of the theoretical calculation is considered as 3% based on conservative estimations from Refs. [24, 25] and 1% assumed to be achieved by the time of the experiments. This follows the same assumption as in Ref. [11]. The 1% and 3% uncertainty on the cross-section will lead to a measurement uncertainty of top quark mass 9 MeV and 26 MeV, which are in the same level of the statistical uncertainty and three times of that, respectively.

The quick scan is used to locate the optimal energy point in advance to the high-luminosity measurement. Several iterations are needed to approach the truth optimal point, the precision of which is limited by the digital step of the beam energy. CEPC has a control on its centre-of-mass energy down to a level of  $10^{-5}$  that leads to an ultimate digital step of 3.5 MeV at around the  $t\bar{t}$  threshold. This is used as a variation on the optimal energy point and is propagated to the top mass measurement, which results in an uncertainty of 3 MeV.

The width and  $\alpha_S$  are fixed to their SM predictions when extracting top quark mass. The uncertainty on top quark mass is up to 17 MeV introduced by a variation of 0.0007 on  $\alpha_S$  [26]. The uncertainty on top quark mass is up to 10 MeV by varying the width of 0.14 GeV taken from the measurement from the CMS result [27].

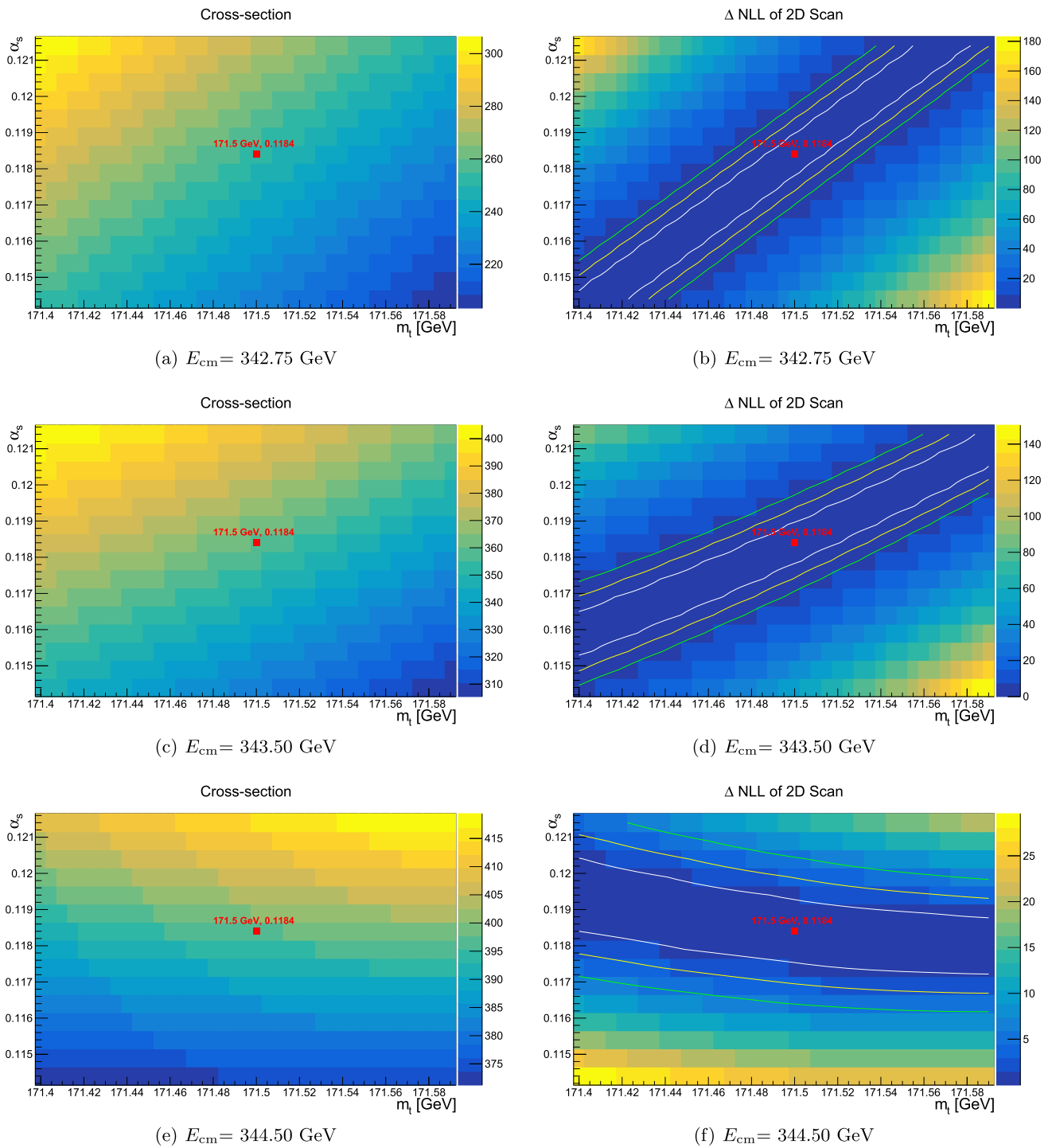


**Fig. 4** The cross-section at certain energy point (left column) and the negative log likelihood at the same energy point (right column) on the plane of top quark mass vs  $\alpha_s$ . The energy points are 342.75, 343.50 and 344.50 GeV. The color shows the cross-section in the left column and the

negative log likelihood values in the right column. The square marker in each plot shows the top quark mass and  $\alpha_s$  used in the expected nominal value. The contour lines in each right plot show the 1, 2 and 3  $\sigma$  bands derived from the likelihood

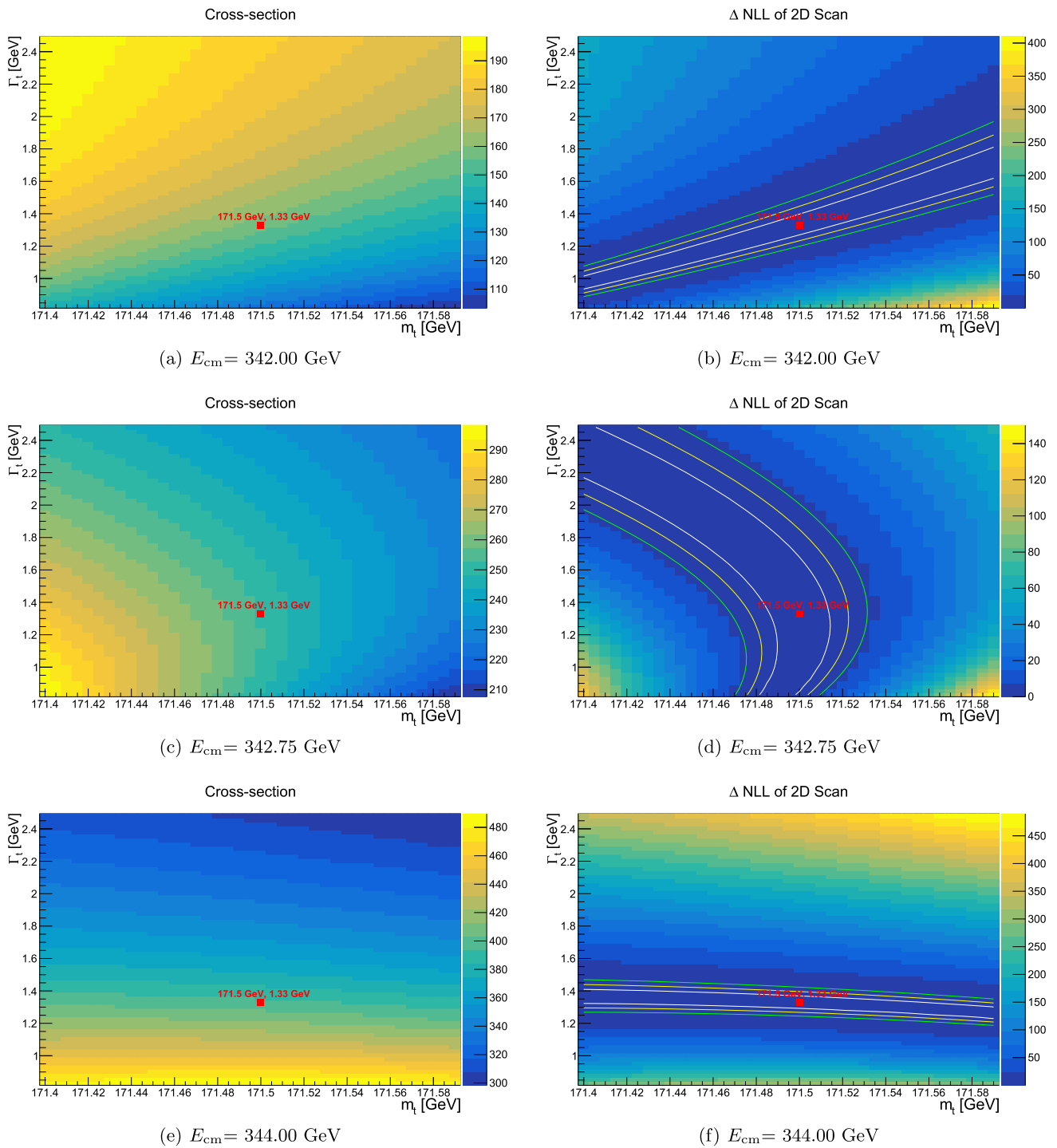


**Fig. 5** The cross-section at certain energy point (left column) and the negative log likelihood at the same energy point (right column) on the plane of top quark mass vs width. The color shows the cross-section in the left column and the negative log likelihood values in the right

column. The square marker in each plot shows the top quark mass and width used in the expected nominal value. The contour lines in each right plot show the 1, 2 and 3  $\sigma$  bands derived from the likelihood



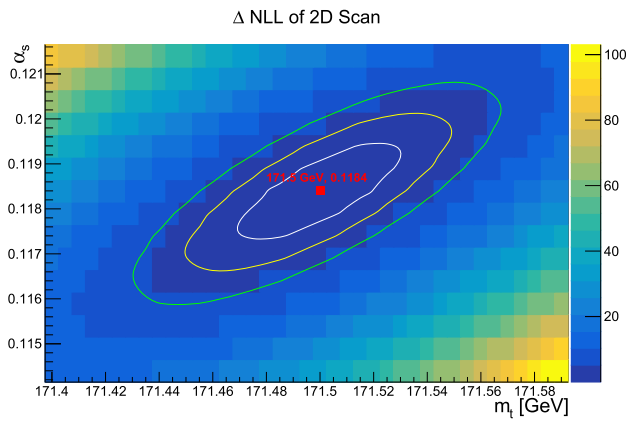


**Fig. 6** The two-dimensional likelihood scan for top quark mass vs  $\alpha_S$  using two energy points optimised for this scenario. The color shows the negative log likelihood values. The square marker shows the top quark mass and  $\alpha_S$  used in the expected nominal value. The contour lines show the 1, 2 and 3  $\sigma$  bands derived from the likelihood

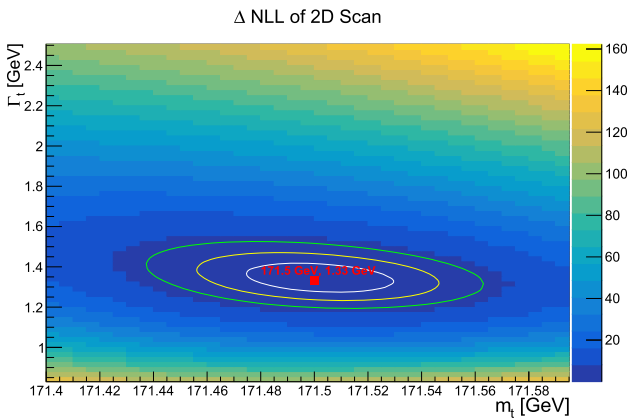


**Fig. 7** The two-dimensional likelihood scan for top quark mass vs width using two energy points optimised for this scenario. The color shows the negative log likelihood values. The square marker shows the top quark mass and width used in the expected nominal value. The contour lines show the 1, 2 and 3  $\sigma$  bands derived from the likelihood

The experimental efficiency of the future detectors are yet to know. We assume several possible scenarios for the level of this uncertainty: 0.5%, 1%, 3% and 5%. This uncertainty impacts directly on the signal yields and results in a measurement uncertainty of the top mass of 5 MeV, 9 MeV, 27 MeV and 45 MeV, respectively.

The background is considered to be subtracted cleanly from the observed data given the good signal-background separation in their shapes, such as the reconstructed top quark mass or a combined kinematic variable, and the statistical dominance of the signal events in the final fitting region. The background uncertainties are added to the likelihood function Eq. 2 as a nuisance parameter constrained by a Gaussian prior. The background efficiencies are taken from Ref. [11], and the cross-sections are calculated at LO including initial-state

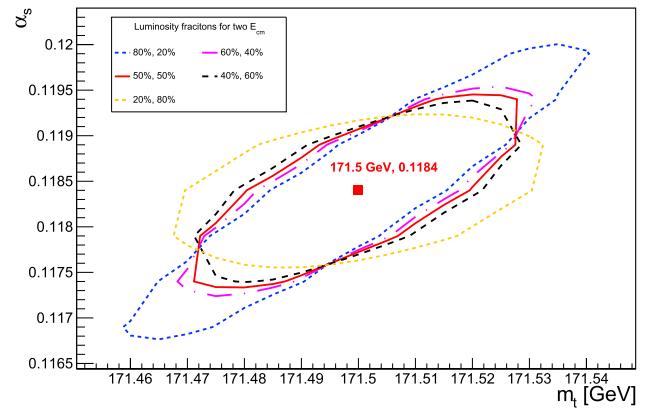


**Fig. 8** The two-dimensional likelihood scan for top quark mass vs  $\alpha_S$  using two energy points optimised for this scenario, using different fractions of luminosity. The square marker shows the top quark mass and  $\alpha_S$  used in the expected nominal value. The contour lines represent the 1  $\sigma$  bands derived from the likelihood. There are five contour lines for the five different schemes of luminosity fractions on the two energy points

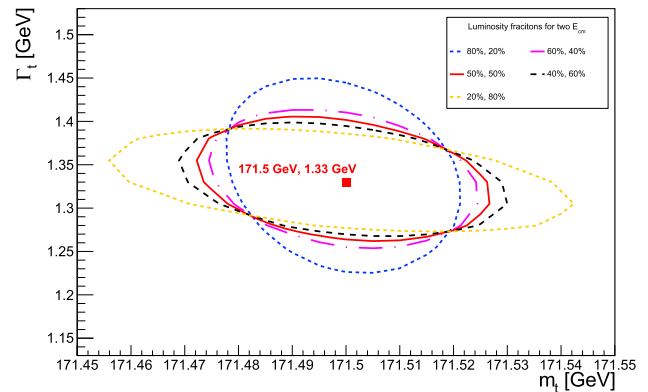


**Fig. 9** The two-dimensional likelihood scan for top quark mass vs width using two energy points optimised for this scenario, using different fractions of luminosity. The square marker shows the top quark mass and width used in the expected nominal value. The contour lines represent the 1  $\sigma$  bands derived from the likelihood. There are five contour lines for the five different schemes of luminosity fractions on the two energy points

radiation with Wizard V1.95 [28,29],<sup>1</sup> as shown in Table 5. Considering the background uncertainty as 1% optimistically and 5% conservatively, a measurement uncertainty of top quark mass of 4 MeV and 18 MeV is reached. From this, the background uncertainty is crucial. Measures like taking data below the threshold to constrain the background might need to be considered.

The variations in the beam energy could also lead to uncertainties on the top quark mass measurement. The beam energy uncertainty was reported at a level of  $10^{-4}$  in the

<sup>1</sup> This estimation is sufficient to get the correct order of magnitude for the background impacts. For a more precise measurement up to NLO + NLL to date, the latest Wizard can be used [30].

**Table 5** Background cross-section near the top threshold and at 500 GeV

$E_{\text{cm}}(\text{GeV})$	352	500
$qq(\text{fb})$	$24149 \pm 69$	$12136 \pm 46$
$W^+W^-(\text{fb})$	$11628 \pm 4$	$7708 \pm 3$
$ZW^+W^-(\text{fb})$	$11.07 \pm 0.01$	$36.16 \pm 0.02$
$ZZ(\text{fb})$	$703.5 \pm 0.3$	$447.9 \pm 0.2$

**Table 6** The expected statistical and systematic uncertainties of the top quark mass measurement in optimistic and conservative scenarios at CEPC

Source	$m_{\text{top}}$ precision (MeV)	
	Optimistic	Conservative
Statistics	9	9
Theory	9	26
Quick scan	3	3
$\alpha_S$	17	17
Top width	10	10
Experimental efficiency	5	45
Background	4	18
Beam energy	2	2
Luminosity spectrum	3	5
Total	25	59

operation of LEP [31, 32] and the studies of ILC [33], which already impacts the top quark measurement less than the statistical uncertainty as discussed in Ref. [11]. In the CEPC scenario, the beam energy could vary 2.6 MeV as estimated from the accelerator team. This impacts the measurement of top quark mass maximally by 2 MeV, way below the statistical uncertainty.

The other aspect from the beam is the uncertainty of the luminosity spectrum. Variations on the spread of the luminosity spectrum, i.e. the width  $\sigma_{LS}$  in Eq. 1, of 10% and 20% are considered. The corresponding uncertainties on the top quark mass measurement are 3 MeV and 5 MeV, respectively. These are quite different than the CLIC scenario in Ref. [11] given the different controls of the luminosity spectrum in circular and linear colliders. Furthermore, the improvement of the top quark mass measurement by having a better luminosity spectrum, e.g. a smaller spread  $\sigma_{LS}$ , is evaluated. The reduction of the energy spread  $\sigma_{LS}$  of 20% and 50% can lead to the statistical uncertainty of top quark mass measurement of 9.0 MeV and 8.4 MeV, with respect to our nominal statistical uncertainty of 9.1 MeV. It appears that a large improvement in luminosity spectrum does not bring much improvement in top quark mass measurement, mostly due to the fact that the majority of the particles in the beams are already constrained

well with a small spread of about 500 MeV at the  $t\bar{t}$  threshold with circular colliders.

Taking into account all these uncertainties, the CEPC is expected to measure the top quark mass with a precision of 25 MeV and 59 MeV in the optimistic and conservative assumptions, respectively, as shown in Table 6.

## 7 Conclusions

We have studied the expected precision of the top quark mass, width and  $\alpha_S$  in  $t\bar{t}$  production using an energy scan around the  $t\bar{t}$  threshold based on the CEPC scenario, assuming a total integrated luminosity of  $100 \text{ fb}^{-1}$ . This study is performed with the package QQbar\_threshold (2.2.0), including the effects of the initial state radiation and the luminosity spectrum.

We focus on a discussion of the measurement with one energy point (two energy points) for the top mass (and the width or  $\alpha_S$ ) with the full luminosity, which turns out to be an efficient way of measurement of the top mass at a high precision. The method of one energy point has a statistical uncertainty with a few MeV better than the scan with multiple energy points. This advantage might be worn out in the process of locating the optimal energy point or possibly large systematic uncertainties from the experimental efficiency. A better understanding of this would require further studies with more realistic uncertainties of the efficiency in the future.

In the one energy point method, measuring one parameter at a time while keeping others to their SM predictions, the precision can reach 9 MeV for top quark mass, 26 MeV for top quark width and 0.00039 for  $\alpha_S$  considering only the statistical uncertainty. The systematic uncertainties from  $\alpha_S$ , width, theory, experimental efficiency and the background subtraction could have the leading impact in the final precision. The systematic uncertainties from the beam energy and the luminosity spectrum influence much mildly. The total uncertainty of top quark mass measurement at CEPC can reach 25 MeV optimistically and 59 MeV conservatively at the optimal centre-of-mass energy. We also discussed measurement of two parameters simultaneously. The scan needs two energy points which should have complementary sensitivity of the two parameters in question. The precision of simultaneous measurements does not exceed the fits with one parameter at a time.

In conclusion, the study shows that CEPC is capable of measuring the top quark mass with a precision below 59 MeV using the single energy point. The method requires a good understanding of theory, experimental efficiency and background estimations, and also requires a low-luminosity scan to locate the optimal energy point.

**Acknowledgements** H. Zhang is pleased to recognize the support and the hospitality of the Center for High Energy Physics at Peking University. Z. Li, Y. Fang, G. Li, S. Xin, S. Wang, Y. Wang, Y. Zhang and Z. Liang are supported in part by Institute of High Energy Physics, Chinese Academy of Sciences under the innovative project on sciences and technologies of no. E2545AU210. H. Zhang is supported in part by the National Science Foundation of China under Grant No. 12075257, by Institute of High Energy Physics, Chinese Academy of Sciences with Contract no. Y6515580U1, and by the funding from Chinese Academy of Sciences with Contract no. Y8291120K2. X. Sun is supported in part by the National Science Foundation of China under Grants no. 12175006 and no. 12061141002, and by Peking University under startup Grant no. 7100603613.

**Data availability statement** This manuscript has no associated data or the data will not be deposited. [Authors' comment:...].

**Open Access** This article is licensed under a Creative Commons Attribution 4.0 International License, which permits use, sharing, adaptation, distribution and reproduction in any medium or format, as long as you give appropriate credit to the original author(s) and the source, provide a link to the Creative Commons licence, and indicate if changes were made. The images or other third party material in this article are included in the article's Creative Commons licence, unless indicated otherwise in a credit line to the material. If material is not included in the article's Creative Commons licence and your intended use is not permitted by statutory regulation or exceeds the permitted use, you will need to obtain permission directly from the copyright holder. To view a copy of this licence, visit <http://creativecommons.org/licenses/by/4.0/>.

Funded by SCOAP<sup>3</sup>. SCOAP<sup>3</sup> supports the goals of the International Year of Basic Sciences for Sustainable Development.

## References

- V.S. Fadin, V.A. Khoze, Threshold behavior of heavy top production in  $e^+e^-$  collisions. *JETP Lett.* **46**, 525–529 (1987)
- V.S. Fadin, V.A. Khoze, Production of a pair of heavy quarks in  $e^+e^-$  annihilation in the threshold region. *Sov. J. Nucl. Phys.* **48**, 309–313 (1988)
- M.J. Strassler, M.E. Peskin, The heavy top quark threshold: QCD and the Higgs. *Phys. Rev. D* **43**, 1500–1514 (1991)
- I.I.Y. Bigi, Y.L. Dokshitzer, V.A. Khoze, J.H. Kuhn, P.M. Zerwas, Production and decay properties of ultraheavy quarks. *Phys. Lett. B* **181**, 157–163 (1986)
- CDF and D0 Collaborations, Combination of CDF and D0 results on the mass of the top quark using up  $9.7 \text{ fb}^{-1}$  at the Tevatron. **8** (2016)
- ATLAS Collaboration, Measurement of the top quark mass in the  $t\bar{t} \rightarrow \text{lepton} + \text{jets}$  channel from  $\sqrt{s} = 8 \text{ TeV}$  ATLAS data and combination with previous results. *Eur. Phys. J. C* **79**(4), 290 (2019)
- C.M.S. Collaboration, Measurement of the top quark mass using proton-proton data at  $\sqrt{s} = 7$  and  $8 \text{ TeV}$ . *Phys. Rev. D* **93**(7), 072004 (2016)
- P.X. Shen, P. Azzurri, C.X. Yu, M. Boonekamp, C.M. Kuo, P.Z. Lai, B. Li, G. Li, H.N. Li, Z.J. Liang, B. Liu, J.M. Qian, L.S. Shi, Data-taking strategy for the precise measurement of the W boson mass with a threshold scan at circular electron positron colliders. *Eur. Phys. J. C* **80**, 66 (2020)
- M.N. Achasov, X. Mo, N.Y. Muchnoi, I. Nikolaev, S.A. Privalov, J.Y. Zhang, Tau mass measurement at bes-iii. *EPJ Web Conf.* **212**, 08005 (2019)
- M. Martinez, R. Miquel, Multiparameter fits to the  $t$  anti- $t$  threshold observables at a future  $e^+e^-$  linear collider. *Eur. Phys. J. C* **27**, 49–55 (2003)
- K. Seidel, F. Simon, M. Tesar, S. Poss, Top quark mass measurements at and above threshold at CLIC. *Eur. Phys. J. C* **73**(8), 2530 (2013)
- T. Horiguchi, A. Ishikawa, T. Suehara, K. Fujii, Y. Sumino, Y. Kiyo, Hi. Yamamoto, Study of top quark pair production near threshold at the ILC. [arXiv:1310.0563](https://arxiv.org/abs/1310.0563) (2013)
- H. Abramowicz et al., Top-quark physics at the CLIC electron-positron linear collider. *JHEP* **11**, 003 (2019)
- A. Abada et al., FCC-ee: the lepton collider: future circular collider conceptual design report volume 2. *Eur. Phys. J. ST* **228**(2), 261–623 (2019)
- A.H. Hoang, What is the top quark mass? *Annu. Rev. Nucl. Part. Sci.* **70**, 225–255 (2020)
- CEPC Study Group, CEPC conceptual design report: volume 1—accelerator. **9** (2018)
- M. Dong et al., CEPC conceptual design report: volume 2—physics and detectors **11** (2018)
- L. Linssen, A. Miyamoto, M. Stanitzki, H. Weerts, Physics and detectors at CLIC: CLIC conceptual design report. **2** (2012)
- M. Aicheler, P. Burrows, M. Draper, T. Garvey, P. Lebrun, K. Peach, N. Phinney, H. Schmickler, D. Schulte, N. Toge, *A multi-TeV linear collider based on CLIC technology: CLIC conceptual design report* (Monographs. CERN, Geneva, CERN Yellow Reports, 2012)
- M. Beneke, Y. Kiyo, A. Maier, J. Piclum, Near-threshold production of heavy quarks with  $Q\bar{Q}$  threshold. *Comput. Phys. Commun.* **209**, 96–115 (2016)
- M. Beneke, A. Maier, T. Rauh, P. Ruiz-Femenia, Non-resonant and electroweak NNLO correction to the  $e^+e^-$  top anti-top threshold. *JHEP* **02**, 125 (2018)
- M. Beneke, Y. Kiyo, K. Schuller, Third-order correction to top-quark pair production near threshold I. Effective theory set-up and matching coefficients. [arXiv:1312.4791](https://arxiv.org/abs/1312.4791) (2013)
- M. Beneke, Y. Kiyo, P. Marquard, A. Penin, J. Piclum, M. Steinhauser, Next-to-next-to-next-to-leading order QCD prediction for the top antitop  $S$ -wave pair production cross section near threshold in  $e^+e^-$  annihilation. *Phys. Rev. Lett.* **115**(19), 192001 (2015)
- M. Stahlhofen, A. Hoang, NNLL top-antitop production at threshold. *PoS* **011**, RADCOR2025 (2011)
- A.H. Hoang, M. Stahlhofen, The top-antitop threshold at the ILC: NNLL QCD uncertainties. *JHEP* **05**, 121 (2014)
- S. Bethke, World summary of  $\alpha_s$  (2012). *Nucl. Phys. B Proc. Suppl.* **234**, 229–234 (2013)
- C.M.S. Collaboration, Measurement of the ratio  $\mathcal{B}(t \rightarrow Wb)/\mathcal{B}(t \rightarrow Wq)$  in pp collisions at  $\sqrt{s} = 8 \text{ TeV}$ . *Phys. Lett. B* **736**, 33–57 (2014)
- W. Kilian, T. Ohl, J. Reuter, WHIZARD: simulating multi-particle processes at LHC and ILC. *Eur. Phys. J. C* **71**, 1742 (2011)
- M. Moretti, T. Ohl, J. Reuter, O'Mega: an optimizing matrix element generator. [arXiv:hep-ph/0102195v1](https://arxiv.org/abs/hep-ph/0102195v1) (2001)
- F. Bach, B.C. Nejad, A. Hoang, W. Kilian, J. Reuter, M. Stahlhofen, T. Teubner, C. Weiss, Fully-differential top-pair production at a lepton collider: from threshold to continuum. *JHEP* **03**, 184 (2018)
- R. Assmann et al., Calibration of centre-of-mass energies at LEP 2 for a precise measurement of the W boson mass. *Eur. Phys. J. C* **39**, 253–292 (2005)
- G. Abbiendi et al., Determination of the LEP beam energy using radiative fermion-pair events. *Phys. Lett. B* **604**, 31–47 (2004)
- S. Boogert et al., Polarimeters and energy spectrometers for the ILC beam delivery system. *JINST* **4**, P10015 (2009)